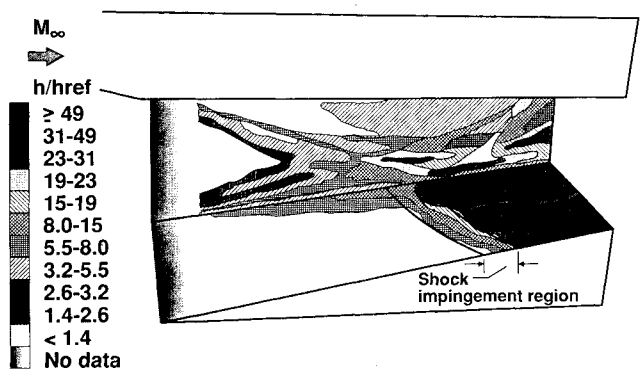

Fig. 2 Heat transfer distribution in the cowl-strut corner (no boundary-layer trips).

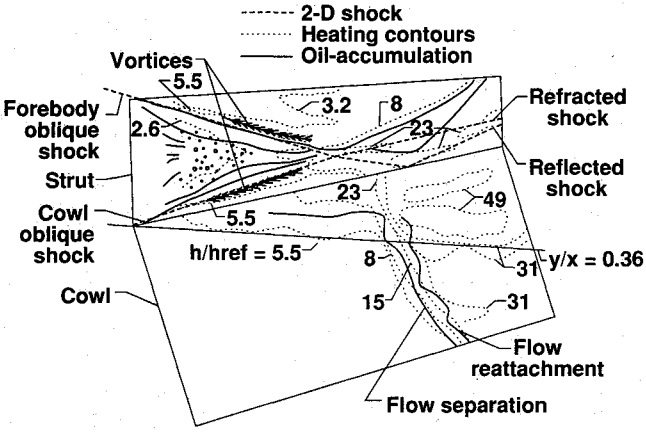

Fig. 3 Two-dimensional shock location and oil-flow lines shown with heating contours (no boundary-layer trips).

peak heating is approximately 50 times the undisturbed laminar reference heating level and on the order of 1.5 times that of the surrounding area downstream of the shock impingement. The h/h_{ref} value of the surrounding area is from 31 to 49. The heating in the vicinity of the corner, upstream of the shock impingement region, is much lower than the peak heating but higher than the heating in the undisturbed regions. The contours on the strut show a lower heat transfer coefficient in the triangular region formed by the strut leading edge and the crossing pattern of the forebody and cowl shock waves. Downstream of the shock interference region, the heating pattern on the strut is extremely complex due to highly three-dimensional flow interactions.

Figure 3 shows the opened-out cowl and strut surface of the model with the same heating contours of Fig. 2. The prominent oil accumulation lines are superimposed on both surfaces for direct comparison with heating contours. On the cowl surface, oil accumulation lines indicating flow separation and reattachment correspond to the region of high heating gradients indicated by the closely spaced heating contour lines. This region is created by the forebody shock impingement on the cowl. The arbitrarily chosen $y/x = 0.36$ line bounds the corner heating contours upstream of the forebody-cowl shock impingement location and the two peak heating regions downstream of the forebody-cowl shock impingement location. On the strut surface, the feather-shaped oil accumulation lines coincide with the two-dimensional inviscid shock lines from the forebody and cowl that are projected on the strut surface. Separated flow in the triangular region, upstream of this forebody-cowl shock crossing pattern, is indicated by the oil-flow pattern. Also, the highest heating rates ($h/h_{ref} = 23$) on the strut surface occurred in the region between the refracted and reflected shock waves.

Similar results (not presented) were obtained with flow trips that produced turbulent level heating ahead of the shock impingement region. Generally, the features of the tripped case were similar to the untripped case, except that the flow separation did not occur on the strut surface upstream of the shock interaction region for the tripped boundary-layer case. Also, the same two peak heating regions occurred on the cowl, and the heating level was about the same as that for the untripped case, indicating that the shock interference heating was independent of the upstream boundary-layer conditions for the present investigation.

Conclusions

The aerodynamic heating in an axial compression corner with an external oblique shock impingement is characterized qualitatively. The local peak heating occurred on the cowl near the corner downstream of the forebody-cowl shock impingement location and was about 50 times the reference undisturbed laminar heating. The peak heating was on the order of 1.5 times that of the surrounding value downstream of the shock impingement. There was no significant difference in the magnitude and location of the peak heating between the untripped and tripped cases.

References

[1]Korkegi, R. H., "Survey of Viscous Interaction Associated with High Mach Number Flight," *AIAA Journal*, Vol. 9, No. 5, 1971, pp. 771–784.

[2]Venkateswaran, S., Witte, D. W., and Hunt, L. R., "Aerothermal Study in an Axial Compression Corner with Shock Impingement at Mach 6," AIAA Paper 91-0527, Jan. 1991.

[3]Keyes, J. W., "Force Testing Manual for the Langley 20-Inch Mach 6 Tunnel," NASA TM-74206, July 1977.

[4]Jones, R. A., and Hunt, J. L., "Use of Fusible Temperature Indicators for Obtaining Quantitative Aerodynamic Heat-Transfer Data," NASA TR R-230, Feb. 1966.

[5]Gillerlain, J. D., Jr., "Use of Phase Change Paints To Study Fin-Body Interference Heating," Naval Surface Weapons Center, NSWC/WOL/TR 75-62, White Oak Lab., Silver Spring, MD, April 1976.

Gerald T. Chrusciel
Associate Editor

Effects of Space Radiation on High-Temperature Superconducting Thin Films of $YBa_2Cu_3O_{7-x}$

Roman Herschitz,* Alexander Bogorad,† Charles Bowman,‡ and Surinder Seehra§
General Electric Company, Princeton, New Jersey 08543
and
Antonio Mogro-Campero¶ and Larry Turner**
General Electric Company, Schenectady, New York 12301

Introduction

HIGH-TEMPERATURE superconducting materials are expected to offer significant improvements in the performance of spacecraft components. Specifically, low surface

Received April 4, 1990; revision received Aug. 13, 1991; accepted for publication Aug. 15, 1991.

*Principal Member of the Technical Staff, Astro-Space Division.
†Member of the Technical Staff, Astro-Space Division.
‡Staff Engineer, Astro-Space Division.
§Manager, Physical Effects Group, Astro-Space Division.
¶Physicist, Research and Development Center.
**Technical Specialist, Research and Development Center.

resistance at high frequencies is expected to result in reduced rf losses in superconducting waveguides, bandpass filters, and antennas.[1-5] From a practical viewpoint, it is important to understand the radiation response of high-temperature superconductors before they can be utilized on any spacecraft components. The primary objective of this Note is to report on space radiation studies performed on thin films of high-temperature superconducting materials.

It is attractive to provide passive cooling to superconductors by locating them on the shaded side of a space vehicle, radiating directly into space. Unfortunately, this technique may result in exposure to high radiation dose levels due to trapped electrons and protons in the space environment. The effects of space radiation on superconducting properties of yttrium barium copper oxide (YBCO) materials are therefore critically important in incorporating these materials into spacecraft systems.

Typically, the space environment consists of ionizing radiation, atomic oxygen, solar (uv) radiation, and solid particles (micrometeoroids). Ionizing radiation includes trapped particles, solar flare particles, and their secondary emissions when they interact with materials. For a given mission, the ionizing radiation intensity varies as a function of solar activity and with the occurrence of geomagnetic storms. The nature of the ionizing environment depends on the trajectory of a given spacecraft. The most comprehensive description of the space radiation environment as a function of altitude in geosynchronous orbit and low Earth orbit is given in Refs. 6 and 7. Earth-orbiting spacecraft encounter trapped electrons and protons in the Earth's geomagnetic belts, where doses to the outer surfaces (within a micron of the surface) often exceed 10^7 rad (Al)/yr for a communications satellite at geosynchronous orbit.[6] For spacecraft orbiting at lower altitudes, such as the Space Station in a 500-km 28-deg inclination, the radiation dosage is 10^4rad(Al)/yr.[7] The total absorbed dose for a given depth of material (aluminum is a common standard) can be predicted for any orbit scenario using the SHIELDOSE computer software program.[8]

It is a standard practice in the aerospace industry to employ 1.25-MeV Co-60 gamma ray source to simulate the radiative effects from the electrons and protons on conventional semiconductor devices. It has been determined that this method is valid for simulation of the ionization damage to the materials.[9,10] This method may not accurately simulate the displacement damage due to heavy ions or damage induced by chemical interactions. However, the effect of these interactions on the superconducting thin films has been published elsewhere.[11-18]

Most of the previously published work presents the effects of heavy ions and high-energy (≥ 2 MeV) electrons and protons. The effects of lower-energy electrons (<1 MeV) on superconducting thin films has not been published.

Our investigation had two objectives: 1) to determine the effects of space radiation on superconducting materials, and 2) to determine whether this effect can be simulated with Co-60 gamma rays, the standard test method for space materials. The effects of atomic oxygen, solar radiation, and solid particles were not part of this investigation.

Experiment

Thin films of YBCO were formed by coevaporation of Y, BaF_2, and Cu and postannealing in wet oxygen at 850°C for 3.5 h. The substrate used was (100) silicon with an evaporated zirconia buffer layer. Processing and microstructure studies of these types of films have been published.[19-22] The zero-resistance transition temperatures of the samples used in this study were 84–86 K. The samples were characterized by four-point probe electrical measurements as a function of temperature. The parameters measured were the zero-resistance transition temperature T_c and the room-temperature resistance. The samples were then exposed to Co-60 gamma rays, in air and in pure nitrogen, and to 780-keV electrons in air, and the parameters were remeasured.

Results

The results, summarized in Tables 1 and 2, indicate little or no degradation in the measured parameters for samples exposed to up to 50 Mrad of gamma rays in nitrogen. However, complete degradation of samples exposed to 10 Mrad in air was observed. This degradation is preliminarily attributed to the high level of ozone generated in the chamber by the gamma-ray interaction with air. Furthermore, no degradation in superconducting properties of samples exposed to 10^{15} electrons at 780 keV in air was observed.

Table 1 Summary of gamma-ray exposures on superconducting materials

Sample description	Ambient environment	Gamma-ray dose, Mrad	Transition temperature, K: Before exposure	Transition temperature, K: After exposure	Comments
YBCO on Si	Air	10	86	—	Catastrophic failure
YBCO on Si	Air	100	85	—	Complete erosion of superconducting film
YBCO on Si	Nitrogen	10	85	84	No degradation in T_c
YBCO on Si	Nitrogen	50	85	84	No degradation in T_c
YBCO on Si with silver pads	Nitrogen	10	86	82	Slight degradation in T_c
	Nitrogen	50	86	81	
YBCO on Si (control sample)[a]	Air	—	85	85	No degradation in T_c (after 21 days)

[a]The control sample was placed outside of the Co-60 source, and its superconducting properties were compared to the exposed samples.

Table 2 Summary of electron exposures on superconducting materials

Sample description	Ambient environment	Electron dose, e^-/cm^2	Transition temperature, K: Before exposure	Transition temperature, K: After exposure	Comments
YBCO on Si	Air	10^{15}	84	84	No degradation in T_c
YBCO on Si (control sample)[a]	Air	—	85	85	No degradation in T_c

[a]The control sample was placed outside of the electron generator, and its superconducting properties were compared to the exposed samples.

Discussion

The radiation tests show that polycrystalline YBCO films on Si are only slightly affected by gamma and electron radiation. Significant changes in the electrical properties of bulk YBCO exposed to 1-MeV electrons have been reported.[23] For these YBCO bulk materials, degradation occurred at a fluence of 6.5×10^{11} e^-/cm^2. We believe that the relatively good performance of our thin films is related to the use of BaF_2 as an evaporation source.

Even though the annealing of thin film is performed in wet oxygen to remove the fluorine from the films, we have found by x-ray photoelectron spectroscopy that about 1 at.% fluorine abundance remains in the surface region. We speculate that the fluorine improves the degradation performance of these films.[24] As suggestive evidence, we cite Tressaud et al.,[25] who found that a thin surface layer containing fluorine provides protection against hydrolysis and gas exchange. It has also been suggested by Mogro-Campero et al.[26] that a thin surface layer containing fluorine improves the resistance of YBCO to degradation caused by thermal cycling.

Conclusions

The following conclusions can be made.

1) The electron component of space radiation does not degrade the critical temperature of the YBCO films described herein, at least for energies around 800 keV and doses similar to those received by surface materials on spacecraft.

2) For qualifying this and other superconducting materials against the space-radiation threat, the standard test method used in the aerospace industry, namely, exposure to Co-60 gamma rays in air, may require some further investigation. The tests that we performed most likely represent a worst-case scenario compared to the tests in a standard space vacuum environment. As a minimum, the sample must be either in vacuum or in positive nitrogen pressure.

The results of this study and that reported by Mogro-Campero et al.[26] are encouraging for the use of YBCO films on satellites because these films resist degradation from radiation and temperature cycling. Thus, even with a lack of protective layers, passive cooling can be provided to the thin YBCO films by exposing them to space without concern about radiation damage.

Acknowledgments

This work was sponsored by the General Electric Internal Research and Development Project. This support is gratefully acknowledged. We also would like to acknowledge useful discussions on space environment with George Brucker.

References

[1]Lyons, W. G., and Withers, R. S., "Passive Microwave Device Applications of High T_c Superconducting Thin Films," *Microwave Journal*, Vol. 33, No. 11, 1990, pp. 94–102.

[2]Withers, R. S., Anderson, A. C., and Oates, D. E., "High-T_c Superconducting Thin Films for Microwave Applications," *Solid State Technology*, Vol 33, No. 8, 1990, pp. 83–87.

[3]Dinger, R. J., "Some Potential Antenna Applications of High-Temperature Superconductors," *Journal of Superconductivity*, Vol. 3, No. 3, 1990, pp. 287–296.

[4]Anon., "High-Temperature Superconductivity in Perspective," U.S. Congress, Office of Technology Assessment, U.S. Government Printing Office, OTA-E-440, Washington, DC, April 1990.

[5]Nisenoff, M., "Space Applications of Superconductivity," *Principles and Applications of Superconducting Quantum Interference Devices*, edited by A. Barone, World Scientific, Singapore, 1990.

[6]Stassinopoulos, E. G., and Barth, J. M., "Charged Particle Radiation Exposure of Geostationary Orbits," NASA Publication X-600-85-12, June 1985.

[7]Stassinopoulos, E. G., and Barth, J. M., "Non-Equatorial Terrestrial Low Altitude Charged Particle Radiation Environment," NASA Publication X-600-87-7, Version 2, Revised Edition, May 1987; also Stassinopoulos, E. G., Barth, J. M., and Smith, R. L., "Space Station Charged Particle Environment Study," NASA Publication X-600-87-6, Nov. 1986.

[8]Seltzer, S. M., "SHIELDOSE: A Computer Code for Space-Shielding Radiation Dose Calculations," National Bureau of Standards, TN 116, Gaithersburg, MD, May 1980.

[9]Stassinopoulos, E. G., Brucker, G. J., Van Gunten, O., Knudson, A. R., and Jordan, T. M., "Radiation Effects on MOS Devices: Dosimetry, Annealing, Irradiation Sequence, and Sources," *IEEE Transactions on Nuclear Science*, Vol. NS-20, No. 3, 1983, pp. 1880–1884.

[10]Everhart, T. E., and Hoff, P. H., "Determination of Kilovolt Electron Energy Dissipation vs. Penetration Distance in Solid Materials," *Journal of Applied Physics*, Vol. 42, No. 13, 1971, pp. 5837–5846.

[11]Parkin, D. M., and Nastasi, M., "Radiation Induced Amorphization in $YBa_2Cu_3O_7$ and $GdBa_2Cu_3O_7$ Superconductors," *Proceedings of the Materials Research Society Meeting*, Materials Research Society, Pittsburgh, PA, Dec. 1988.

[12]Nastasi, M., Parkin, D. M., Zocco, T. G., Koike, J., and Okamoto, P. R., "Electron Irradiation Induced Amorphization in $YBa_2Cu_3O_7$," *Applied Physics Letters*, Vol. 53, No. 14, 1988pp. 1326–1328.

[13]Egner, B., Geerk, H., Li, H. C., Linker, G., Meyers, O., and Strehlau, B., "The Influence of Irradiation-Induced Defects on the Superconductivity of $YBa_2Cu_3O_7$," *Japanese Journal of Applied Physics*, Vol. 26, No. 7, 1987, pp. 2141, 2142.

[14]VanDover, R. B., Gyorgy, E. M., Schneemeyer, L. F., Mitchell, J. W., Rao, K. V., Puzniak, R., and Waszczak, J. V., "Critical Currents near 10^6 Acm^{-2} at 77K in Neutron-Irradiated Single-Crystal $YBa_2Cu_3O_7$," *Nature*, Vol. 342, No. 6245, 1989, pp. 55–57.

[15]Sumners, G. P., Burke, E. A., Chrisey, D. B., Nastasi, M., and Tesmer, J. R., "Effect of Particle-Induced Displacements on the Critical Temperature of $YBa_2Cu_3O_{7-x}$," *Applied Physics Letters*, Vol. 55, No. 14, 1989, pp. 1469–1471.

[16]Masegi, T., Terai, T., Takahasri, Y., Enomoto, Y., and Kubo, S., "Effects of Ion Irradiation on the Critical Current Density of $Ba_2YCu_3O_{7-x}$ Thin Films," *Journal of Applied Physics*, Vol. 9, No. 8, 1989, pp. L1521–1523.

[17]Roas, B., Hensel, B., Henke, S., Klaumunzer, S., Kabius, B., Watanabe, W., Saeman-Ischenko, G., Schultz, L., and Urban, K., "Effects of 173 $MeV_{129}Xe$ Ion Irradiation on Epitaxial $YBa_2Cu_3O_x$ Films," *Europhysics Letters*, Vol. 11, No. 7, 1990, pp. 669–674.

[18]Gromov, V. V., Karaseva, L. G., Kozlov, V. A., Lukhin, A. S., Rozno, A. G., and Khodyakov, A. A., "The Influence of the Gaseous Medium on the Superconducting Properties of the Gamma-Irradiated $YBa_2Cu_3O_{7-x}$ Ceramic," *Russian Journal of Physical Chemistry*, Vol. 64, No. 4, 1990, pp. 574–575.

[19]Mogro-Campero, A., Turner, L. G., Hall, E. L., and Burrell, M. C., "Characterization of Thin Films of YBaCuO on Oxidized Silicon with a Zirconia Buffer Layer," *Applied Physics Letters*, Vol. 52, No. 24, 1988, pp. 2068–2070.

[20]Mogro-Campero, A., Turner, L. G., and Kendall, G., "Thickness and Annealing Dependence of the Superconducting Transition Temperature of $YBa_2Cu_3O_{7-x}$ Thin Films on Oxidized Silicon and Polycrystalline Alumina Substrates," *Applied Physics Letters*, Vol. 53, No. 25, 1988, pp. 2566–2568.

[21]Mogro-Campero, A., Turner, L. G., and Hall, E. L., "Large Differences of Critical Current Density in Thin Films of Superconducting $YBa_2Cu_3O_{7-x}$," *Journal of Applied Physics*, Vol. 65, No. 12, 1989, pp. 4951–4954.

[22]Mogro-Campero, A., Turner, L. G., Hall, E. L., Garbauskas, M. F., and Lewis, N., "Epitaxial Growth and Critical Current Density of Thin Films of $YBa_2Cu_3O_{7-x}$ on $LaAlO_3$ Substrates," *Applied Physics Letters*, Vol. 54, No. 26, 1989, pp. 2719–2721.

[23]Aden, R., Martinez, L., Rickards, J., Orozco, E., Fuentes-Maya, J., Albarran, J. L., Mendoza, A., Carrillo, E., Cota, L., Reyes-Gasga, J., Boldu, J. L., Perez, R., Perez-Ramirez, J. G., and Jose-Yacaman, J., "The Effects of Electron Irradiation in High-T_cOxide Superconductors," *Journal of Materials Research*, Vol. 3, No. 5, 1988, pp. 807–810.

[24]Mankiewich, P. M., Scofied, J. H., Scopol, W. J., Howard, R. E., and Dayem, A. M., "Reproducible Technique for Fabrication of Thin Films of High Transition Temperature Superconductors," *Applied Physics Letters*, Vol. 51, No. 21, 1987, pp. 1183–1188.

[25]Tressaud, A., Chevalier, B., Lepine, B., Dance, J. M., Lozano, L., Grannee, J., Etourneau, T., Tournier, R., Suplice, A., and Lejey, P., "Passivation Process of High-T_c Superconducting $YBa_2Cu_3O_{7-x}$ by Fluorine Gas Treatment," *Modern Physics Letters*, Vol. B2, No. 10, 1988, pp. 1183–1188.

[26]Mogro-Campero, A., Turner, L. G., Bogorad, A., and Herschitz, R., "The Effects of Temperature Cycling on Thin Films of $YBa_2Cu_3O_7$," *Superconducting Science and Technology*, Vol. 3, No. 11, 1990, pp. 537-539.

Paul F. Mizera
Associate Editor

Optical Intensity Fluctuations in Re-Entry Object Observations

R. L. Henry*
Air Force Systems Command, Wright-Patterson Air Force Base, Ohio 45433

Nomenclature

A = projected area of source, m^2
$C_1(0)$ = log-amplitude variance of radiation (dimensionless)
C_2 = second radiation constant, K μm
C_N^2 = atmospheric index-of-refraction structure constant, $cm^{-2/3}$
h = altitude, km
h_t = altitude of tropopause, km
I_1, I_2 = intensity of radiation at wavelengths, λ_1 and λ_2, respectively, W/sr μm
k = wavevector of radiation, cm^{-1}
T = color temperature of source, K
v = integration variable, km
Z = length of viewing path, km
δT = color temperature fluctuation amplitude, K
$\delta\epsilon A$ = emissivity area fluctuation amplitude, m^2
ϵ = emissivity of source (dimensionless)
σ = integration variable, cm^{-1}
$\sigma I_1^2, \sigma I_2^2$ = variances of intensity of radiation at wavelengths, λ_1 and λ_2, respectively, W/sr μm

Introduction

OPTICAL radiation is one source of information on re-entry phenomena. When a re-entering object is observed through the atmosphere, turbulence in the atmosphere between the observer and the re-entering object will induce fluctuations in the observed optical intensity. If data from multiple wavelengths are used to calculate the apparent color temperature of the re-entry object, these intensity fluctuations will result in fluctuations in the calculated color temperature. Conclusions based on optical measurements can be significantly degraded or distorted if these atmosphere-induced effects are not properly interpreted.

The mechanism by which atmospheric turbulence affects the propagation of an optical signal has been well covered in the literature.[1-3] Unfortunately, this theory is usually applied to the case of a ground-based observer looking to space. When the observer is in an aircraft looking at an object that is also in the atmosphere, these effects can be much different. This Note describes the affects of atmospheric turbulence on the observation of a re-entering object when viewed by aircraft-mounted optical instruments. For simplicity, this discussion will be confined to measurements in the visible and near-infrared portion of the spectrum.

Received Aug. 13, 1990; revision received June 6, 1991; accepted for publication June 21, 1991. This paper is declared a work of the U.S. Government and is not subject to copyright protection in the United States.

*Aerospace Engineer, Foreign Technology Division. Associate Fellow AIAA.

Influence of Atmospheric Turbulence

The normalized variance of the intensity of emissions from a point source, when viewed by an instrument with an infinitesimally small point aperture and an infinitesimally short exposure time,

$$\frac{\sigma I^2}{I^2} = \frac{\langle (I - \langle I \rangle)^2 \rangle}{\langle I \rangle^2} \tag{1}$$

is given by

$$\frac{\sigma I^2}{I^2} = \exp\left[4C_1(0)\right] - 1 \tag{2}$$

where[2]

$$C_1(0) = 65{,}200\, k^2 \int_{\substack{\text{Path of} \\ \text{propagation}}} C_N^2 \int_0^\infty \sigma^{-8/3} \times \left[1 - \cos 10^5 \frac{\sigma^2 v(Z - v)}{kZ}\right] d\sigma\, dv \tag{3}$$

These intensity fluctuations are caused by turbulence-induced atmospheric temperature fluctuations that cause density and hence index-of-refraction fluctuations in the viewing path. When a beam propagates along a path that includes regions of strong turbulence, multiple scattering effects cause the magnitude of turbulence-induced fluctuations to saturate.[3] This saturation occurs when the value of σ_I/I predicted by Eqs. (2) and (3) exceeds roughly 3.16.

Consider the effects these intensity fluctuations have on the calculation of the color temperature of the object radiation from measurements in two spectral bands. For simplicity assume that these bands are in the visible spectrum and are sufficiently narrow that their width may be disregarded. This wavelength region is appropriate for optical measurements of re-entry objects because it lies near the peak of the spectral distribution of the surface emissions of common heatshield materials (such as carbon or silica phenolic) during the peak-heating portion of suborbital re-entry trajectories. Under these conditions, the Wein law is a good approximation to Planck's law. Since the mechanism responsible for these fluctuations should affect the entire optical region of the spectrum, a high degree of correlation should be present in the fluctuations observed at different wavelengths when the fluctuations are below the saturation level. Accounting for these correlations, the normalized amplitude of the calculated color-temperature fluctuations is given by

$$\frac{\delta T}{T} = \frac{-T}{C_2(1/\lambda_1 - 1/\lambda_2)} \left(\frac{\delta I_{\lambda 1}}{I_{\lambda 1}} - \frac{\delta I_{\lambda 2}}{I_{\lambda 2}}\right) \tag{4}$$

Notice that the amplitude of the fluctuations in the calculated color temperature is itself temperature-dependent. The corresponding amplitude of the fluctuations in the calculated normalized emissivity area product of the source is given by

$$\frac{\delta \epsilon A}{\epsilon A} = \frac{1}{(\lambda_1 - \lambda_2)} \left(\lambda_1 \frac{\delta I_{\lambda 1}}{I_{\lambda 1}} - \lambda_2 \frac{\delta I_{\lambda 2}}{I_{\lambda 2}}\right) \tag{5}$$

To illustrate these effects, consider the case of an optical package mounted in an aircraft observing a re-entry object at a slant range of 277.5 km. The altitude profile of C_N^2 is weather-dependent. For the purposes of these calculations, assume that C_N is equal to the constant value 3.55×10^{-10} $cm^{-1/3}$ in the troposphere. Further assume that the stratospheric values are given by

$$C_N = 3.55 \times 10^{-10} (h/h_t)^{-0.873}\ cm^{-1/3} \tag{6}$$